VIII. Martian Cratering IV: *Mariner 9* Initial Analysis of Cratering Chronology

William K. Hartmann

Planetary Science Institute, Tucson, Arizona 85704

A. Review of Martian Cratering Analyses

Öpik (Ref. VIII-1) and Tombaugh in *American Astronomer's Report* (Ref. VIII-2) surmised that craters might be abundant on Mars. Craters on Mars were proven to exist through photography by *Mariner 4* in mid-1965. In the first analysis of these pictures by Leighton et al. (Ref. VIII-3), it was pointed out that the crater density of the Martian terrain photographed resembled "remarkably closely the lunar uplands." On this basis, Leighton et al. concluded that the age of the surface was 2 to 5 aeons. Immediately following this, Witting et al. (Ref. VIII-4), Anders and Arnold (Ref. VIII-5), and Baldwin (Ref. VIII-6) pointed out that the Martian cratering rate must be higher than the lunar rate and that the age should be appropriately reduced. The three papers gave ratios of Martian to lunar cratering rates of 15, 25, and 5 to 10, respectively, and all derived ages of the Martian craters in the range 0.3 to 0.8 aeon, about one-tenth the initial estimate.

The next generation of crater studies, still based on *Mariner 4* results, revised the age upward to the original estimate. This resulted primarily from utilizing new crater counts on improved *Mariner 4* pictures, from correcting the lunar crater counts which were being used as a reference, and from correcting the erroneous assumption that surface age could be scaled linearly in proportion to the crater density on Mars expressed as a fraction of the crater density on the ancient lunar uplands. The latter assumption is incorrect because the pre-mare lunar cratering rate was much higher than the post-mare lunar cratering rate, which has been more uniform and thus allows better age scaling. Binder (Ref. VIII-7), Hartmann (Ref. VIII-8), and Öpik (Ref. VIII-9) referenced their counts to assumed lunar mare ages of 4.5, 4, and 4.5 aeons (later radiogenic dates from *Apollo* and *Luna* samples: 3 to 4 aeons) and derived ages for the largest Martian craters of 2.2 to 3, 3.6, and >3 aeons, respectively. Hartmann and Öpik pointed out that impact velocity on Mars was different from that on the Moon and applied a correction factor.

With the publication of these papers, agreement appeared to be reached on the essentials of age estimation based on craters and on the result that the large craters

were several aeons old and not post-Cambrian in age. Discussion in the literature at this point turned to effects of erosion and the state of crater preservation. Hartmann (Ref. VIII-8) had pointed out that the mean or maximum age of a group of craters of a given size was strongly size dependent, using the term "crater retention age" for the age of the oldest crater of any given size in the given geologic province. He concluded that many craters smaller than diameter $D = 50$ km had been obliterated by erosion or filling, but that larger craters gave a crater retention age, indicating the late stages of planet accretion. Öpik (Ref. VIII-9) similarly concluded that the largest craters had survived from the end of a primeval period of intense cratering, but that many smaller craters had been erased by eolian erosion acting at one-thirtieth the rate found in terrestrial deserts. Binder (Ref. VIII-7) also called for "large-scale subaerial erosion" in the early history of Mars, to account for depletion of craters smaller than $D = 40$ km, and related this result to spectrometric evidence for weathered, oxidized iron minerals that imply a denser atmosphere in the past.

Marcus (Ref. VIII-10) also analyzing *Mariner 4* data, found depletion of craters smaller than about 20 to 30 km, and concluded that the surface was nearly saturated with larger craters. Chapman et al. (Refs. VIII-11 and VIII-12) found that the observed craters were degraded in form and made a comprehensive study of the effect of erosive processes on the morphologies of craters and their diameter distribution. These authors concluded that cratering of Mars had produced a cumulative total of 0.1 to several kilometers of dust, and that either extensive crater overlap or erosion transport processes were required to account for the observed morphologies and diameter distribution. In their more detailed paper, Chapman et al. (Ref. VIII-11) derived a dust-filling model for crater obliteration which predicted a series of crater morphologies close to that observed.

At this time, only 0.5% of the Martian surface had been photographed at high resolution, as pointed out most clearly by Öpik (Ref. VIII-9). Most authors implied that since cratering was an external process and the *Mariner 4* pictures cut a long swath across Mars, the cratering could be expected to be similar in most regions. Other cautions were sounded at this time. Binder (Ref. VIII-13) criticized the counts of Chapman et al. (Ref. VIII-11), Marcus (Ref. VIII-10), and Leighton et al. (Ref. VIII-14) for including many small craters which were not confirmed in comparison of their separate counts. Chapman et al. (Ref. VIII-12) pointed out in reply that these small craters had little effect on the crater density

analyses, which were based on the better determined large craters. Wells and Fielder (Ref. VIII-15) criticized Öpik's (Ref. VIII-9) assumption (and that of the other authors) that the craters being analyzed were principally astroblemes. In retrospect, we note that while recent *Mariner* results have disclosed large volcanic calderas, the *Mariner 4* pictures portrayed what is now known to be a heavily cratered part of Mars in which impact craters are believed to predominate. In summary, it appears that *Mariner 4* analyses yielded a valid and consistent picture of a geologically ancient surface with some erosion effects.

Russell and Mayo (Ref. VIII-16), pursuing an early suggestion by Öpik (Ref. VIII-1) and Tombaugh (Ref. VIII-2), measured the size distribution of Martian oases and concluded that they were impact sites. This has not been confirmed by recent data; Juventae Fons and Lunae Lacus, for example, are chaotic terrain collapse sites; Trivium Charontis is not marked by any usual structure; and other classical oases are of less certain nature. Some oases may be dark patches formed in crater floors.

In mid-1969, the second generation of close-up images of Mars became available with far-encounter and near-encounter picture sequences by *Mariners 6* and *7*. By chance, these two spacecraft took nearly all of their near-resolution images in the highly cratered portions of Mars, as did *Mariner 4*. Furthermore, the far-encounter pictures were taken at a low phase angle and considerably poorer resolution than the high-resolution views. For these reasons, the *Mariner 6* and 7 crater analyses were similar in result to those of *Mariner 4*; neither produced any radical change in the conception of Martian cratering, nor did more than hint at the remarkable heterogeneity later revealed by the *Mariner 9* mission. The principal new relevant results were additional support for the hypothesis of past erosion and suggestions that this erosion, evidence for collapse-induced "chaotic terrain," occurred not at a constant or smoothly changing rate, but in episodic events.

In the preliminary analysis of *Mariner 6* and 7 data, Leighton et al. (Ref. VIII-17) conclude that "several billion years" would be required "to produce the density of large craters . . . in the more heavily cratered areas." This is the first recognition of the differences in crater density from one province to another. Murray et al. (Ref. VIII-18), in the final *Mariner 6* and 7 report, studied not only crater numbers but also crater morphology, and reached a number of important conclusions:

(1) Little correlation exists between crater density and classical albedo markings.

(2) Small craters are morphologically different from big craters, being more bowl-shaped.

(3) Large craters date back to a very early period.

(4) Horizontal transport of material is much greater on Mars than on the Moon and affects the crater forms.

(5) Past erosion processes on Mars may have been episodic.

These conclusions are supported by the present *Mariner 9* analysis. Conclusions reached by Murray et al. (Ref. VIII-18), which differ from those reached here, include:

(1) "Craters are the dominant landform on Mars."

(2) "The size-frequency distribution of impacting bodies that produced the present Martian bowl-shaped craters differs from that responsible from post-mare primary impacts on the Moon . . ."

Subsequent analyses of data from *Mariners 6* and *7* focused on the implications of past erosion history on Mars. Hartmann (Ref. VIII-19) found that the diameter distribution of the craters and dynamics of orbital encounter were consistent with impacts by the asteroid population near Mars and required much greater cratering rates and erosion rates in early Martian history. Hartmann (Ref. VIII-20) suggested that a major agent obliterating craters was the deposition of windblown dust in crater floors. McGill and Wise (Ref. VIII-21) found localized differences in small-crater populations and proposed "general continuity of crater formation and degradation with locally sporadic formation and/or degradation of the smallest craters visible."

Oberbeck and Aoyagi (Ref. VIII-22) opened a new area of investigation by proposing that the incidence of doublet craters (nearly tangent to each other) was much higher than random. Such doublets were compared to the terrestrial examples of Clearwater Lake East and West, in Canada, and were attributed to the breakup of incoming meteoroids by tidal stresses set up during passage through the gravitational field of Mars. This hypothesis has not yet been widely studied.

At the beginning of the *Mariner 9* mission then, there was consensus on the following points:

(1) In heavily cratered regions, the oldest large craters ($D \gtrsim 50$ km) date back 3 to 4.5 aeons.

(2) The earliest history of Mars (some 10^8 years?) was marked by intense bombardment associated with accretion.

(3) More erosion and/or obliteration of craters occurred on Mars in the past than is occurring now, and this erosion may have either been concentrated in the earliest history, occurred in sporadic episodes, or both.

(4) Local variations in cratering from region to region exist, but were believed to be relatively minor.

B. Significance of Crater Morphology

At the outset of any discussion of cratering on Mars, it is crucial to determine the relation between the Martian craters and similar features on Earth and the Moon. Only if the features are related can we use them to understand the evolutionary state of the Martian crust vis-a-vis that of Earth and the Moon; i.e., only then can we capitalize on the *Mariner 9* opportunity to practice comparative planetology. Therefore, it is the purpose here to demonstrate that Mars exhibits a sequence of crater forms which matches a sequence found on both Earth and the Moon.

A comparison of crater forms on the three planets is complicated by the undoubted presence on Mars of large volcanic craters. The most clearcut examples, such as those near Phoenicis Lacus and Nix Olympica, lie on the summits of volcanic mountains, large even by terrestrial standards. In these cases, identification of volcanic origin is simple because of characteristics such as summit location, scarps, coalescing rims, and other morphologic features. The largest of these volcanic summit calderas is that near Phoenicis Lacus, having a diameter of about 125 km. The diameter of the caldera on Nix Olympica is about 72 km. This raises a question whether similar sized calderas could appear in abundance in other parts of the planet and be mistaken for impact craters. However, the clear diagnostic characteristics of these volcanic craters, the fact that the Martian craters taken in toto match the diameter distribution predicted for impact of asteroid fragments (see later part of this section), and the frequent indications of ejecta blankets suggest that impact craters predominate and that volcanic craters on Mars, at least at the multi-kilometer size ranges considered here, do not constitute the majority of craters.

Figure VIII-1 shows a size comparison of craters of various morphologic types found on Earth, Mars, and
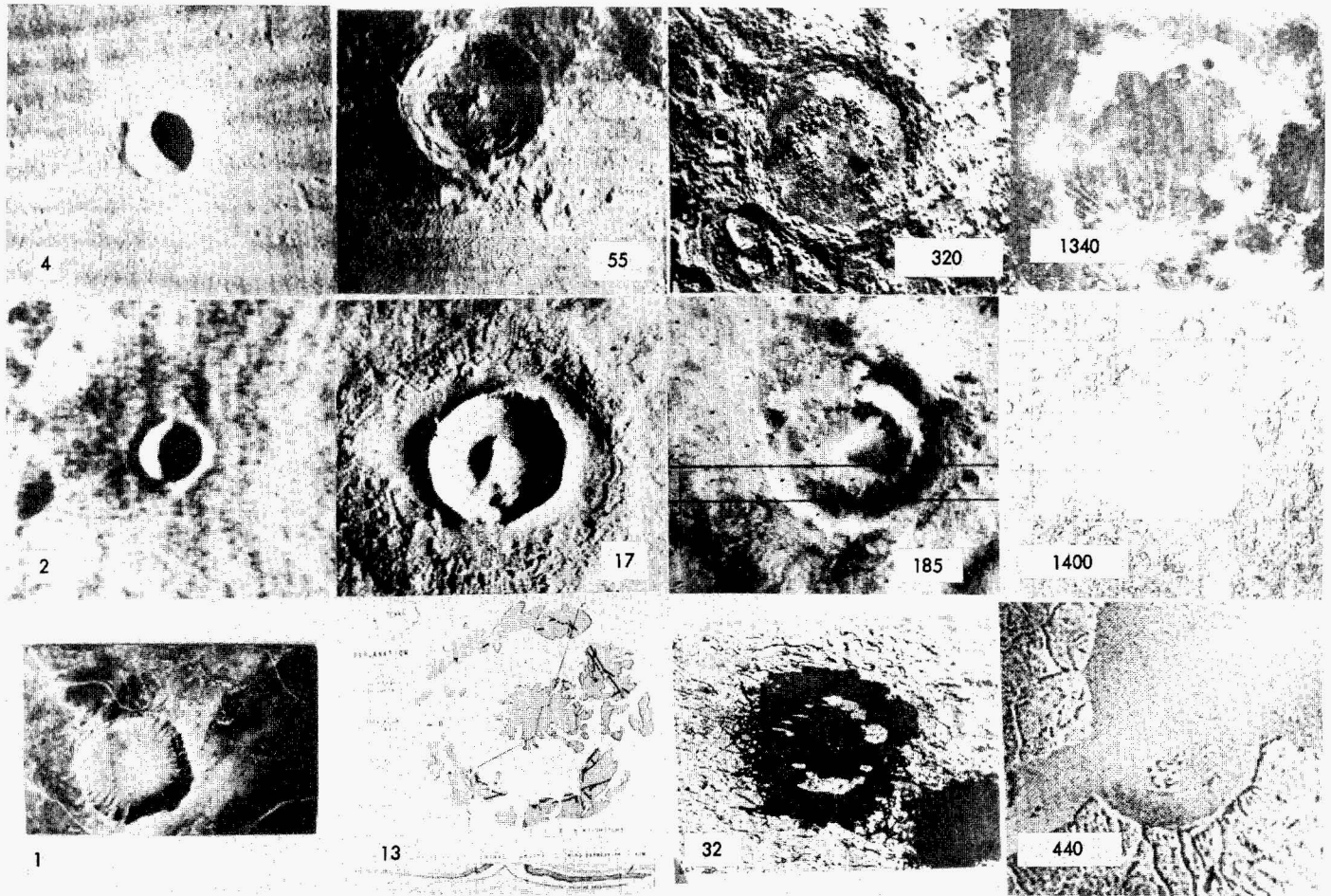
Fig. VIII-1. Comparison of crater types on Moon (top), Mars (middle), and Earth (bottom) showing four types of crater morphology. Diameter in kilometers is given in boldface numbers. Crater types from left to right are bowl-shaped, central peaks, interior ring of peaks, and large basin.

the Moon. If the extensive data on lunar craters are fitted together with field geologic data from studies of terrestrial craters (e.g., Dence et al. in Ref. VIII-23, p. 339), it is evident that a range in crater form exists starting at small diameters with simple bowl-shaped craters, proceeding through what Dence termed complex craters with central uplifts or peaks, and extending to lunar examples of craters with rings of peaks on the crater floor, an example being the crater Schrödinger. At still larger diameters, all manifestations of central mountains disappear and the crater rim is surrounded by a series of concentric ring faults. These concentric systems are not prominent on Mars or Earth, and on the Moon the older examples are severely eroded.

Figure VIII-2 compares the sizes of these crater types on three planets. On Earth, craters as small as 10 km

commonly have central uplifts; on the Moon, the central peak frequency is maximized nearer a diameter of 90 km. Similarly, there is an offset in mean size for other properties, as pointed out in an earlier paper by Hartmann (Ref. VIII-24) based on data from *Mariners 6* and *7*. The *Mariner 9* data confirm the basic observation of the earlier paper, namely that each crater type occurs at smaller physical dimension as the planet grows larger. In the earlier paper, this was attributed to the fact that as surface gravity increases, a smaller volume of rock suffices for gravitational adjustments to overcome the constant strength of rocky material.

It is concluded that similarities exist in basic crater morphology between Martian, lunar, and terrestrial examples, and that most of the larger craters can be compared on the basis of impact theory.
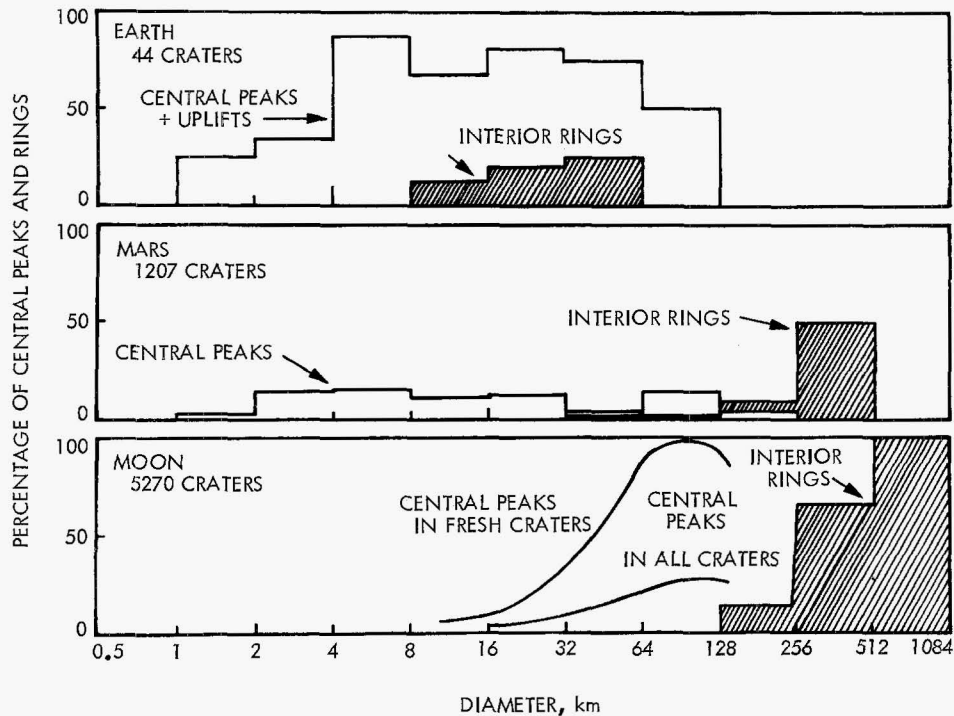
Fig. VIII-2. Histogram showing frequency of occurrence of central peaks and interior rings as a function of diameter for craters on Earth, Mars, and the Moon. Smaller surface gravity results in larger dimension for transition from central peaks to interior rings.

C. Undersaturation: Fossil Record of Asteroid Mass Distribution

The asteroids, which may be related to the population of objects impacting Mars, nearly fit a regular power-law distribution in mass or diameter, except at large sizes, as first pointed out by Kuiper et al. (Ref. VIII-25) and recently confirmed by Van Houten et al. (Ref. VIII-26). The irregularities in mass distribution of large asteroids should be transformed into irregularities in the distribution of large craters on Mars, if most of the Martian craters are caused by asteroidal impacts. The irregularity in question is a flattening of the asteroid size distribution between asteroid diameters of approximately 7 and 50 km.

By converting the asteroid mass distribution into the distribution of crater diameters that would be produced on Mars by asteroid impacts, Hartmann (Ref. VIII-19) predicted that "asteroidal impact craters, if they fall below the saturation line, would show a plateau or flat spot in the crater diameter distribution in approximately the interval $50 < D < 500$ km." The 1971 paper compared the predicted crater distribution with a small sample of craters from *Mariner 4, 6,* and *7* cratering data. Statistical scatter was large among the crater sizes considered, but it was concluded that "the Martian craters do show at

least marginal evidence of the fossil imprint of the asteroid mass distribution." *Mariner 9* data extend the cratering statistics to such a large sample that a much more meaningful comparison can be conducted.

The first problem that must be solved is that of saturation. If true saturation were approached, the diameter distribution of craters would be highly restricted because the diameter distribution would be determined by the maximum geometric packing of craters. Therefore, it is important to guarantee that the areas studied are free from this saturation effect. *Mariner 4, 6,* and *7* pictures all showed regions where the crater density was quite high. *Mariner 9* pictures have clearly shown that some provinces on Mars are sparsely cratered, undersaturated, and apparently young. Thus, it is possible to select regions where saturation is not important and to test for saturation in other regions.

This has been done in the following way: A crater catalog of all craters down to 64 km has been prepared using *Mariner* pictures and preliminary USGS Mars photomosaic charts for latitudes south of +32° where the north polar haze is not an obscuring influence. The catalog was checked against the USGS airbrush structural map with the result that some 30 craters were

added, bringing the total to 550 craters. To define three provinces, the charts were divided into three groups: sparsely cratered, moderately cratered, and heavily cratered. Only the heavily cratered province approaches saturation. Therefore, we have at least two independent groups of data to determine the size distribution of craters in unsaturated regions, and a test for the asteroidal mass distribution can be attempted.

Figure VIII-3 shows the diameter distributions (in logarithmic increments) for craters in the three types of
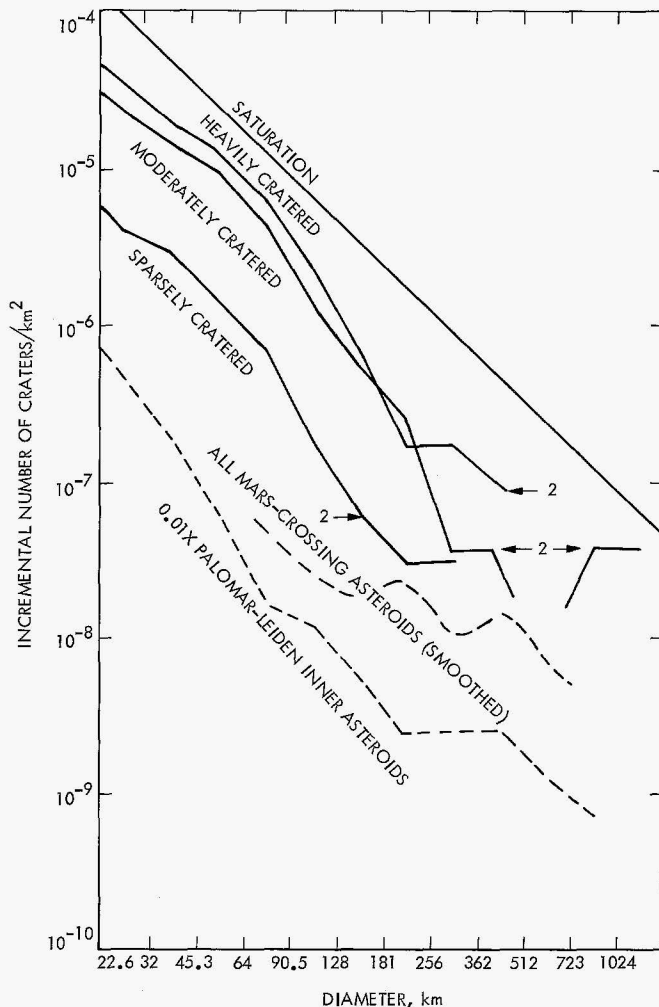

Fig. VIII-3. Comparison of observed diameter distributions of craters on Mars (solid lines) with predicted diameter distributions caused by impacts of all Mars-crossing asteroids (upper dashed line) and 1% of the "inner asteroids" in the Palomar–Leiden survey (lower dashed line). Uppermost curve is the empirical saturation limit. The observed Mars curves show some flattening at large diameters as would be predicted from the asteroids, but the statistics involve very small numbers. The level corresponding to two craters in a single logarithmic diameter increment is indicated by arrows on each curve.

provinces mentioned. Data from the crater catalog for $D > 64$ km are fitted to counts from individual pictures for $D < 64$ km. The upper envelope for all curves is the saturation line, which is based on data from the most heavily cratered lunar uplands and from experiments. Below the three curves showing Martian provinces are predicted diameter distributions for arbitrary numbers of asteroid impacts based on the recent Palomar–Leiden asteroid survey (Ref. VIII-26) and other sources, discussed by Hartmann (Ref. VIII-19). Figure VIII-3 is thus an updated version of Figure 1 of Ref. VIII-19. The asteroid counts can be adjusted by vertical sliding according to the total density of craters considered.

On the basis of the earlier discussion, it had been hoped that *Mariner* 9 would produce a large enough sample of craters so that the fossil record of asteroid mass distribution could be detected or refuted. However, this would have required a large crater sample, i.e., that all of Mars be cratered to the same density as found in the *Mariner 4, 6,* and *7* regions. Instead, as indicated in Fig. VIII-3, large regions are sparsely cratered and the statistics are insufficient to settle the question. The numerals "2" in Fig. VIII-3 indicate, for each curve, where the number of craters in the logarithmic increment drops to two.

The conclusions reached on the basis of Fig. VIII-3 are:

(1) Even the heavily cratered regions of Mars are not saturated with craters.

(2) At $D \gtrsim 100$ km, the Martian craters are quite consistent with known asteroid statistics.

(3) Although the slope of the size distribution of craters flattens or becomes more positive with increasing size in the size range $D > 181$ km, as predicted from comparison with asteroid mass distributions, the absolute numbers of craters are too small to allow a definite conclusion as to correlation or noncorrelation with the asteroid mass distribution.

(4) No data are inconsistent with asteroid impacts.

D. Implication of Hemispheric Asymmetry in Crater Density

Figure VIII-4 shows a Mercator plot of large Martian craters based on the above-mentioned catalog of all craters of $D > 64$ km. The plot reveals a crustal asymmetry. The hemisphere centered south of Deucalionis Regio is heavily cratered, and contains the Hellas, South
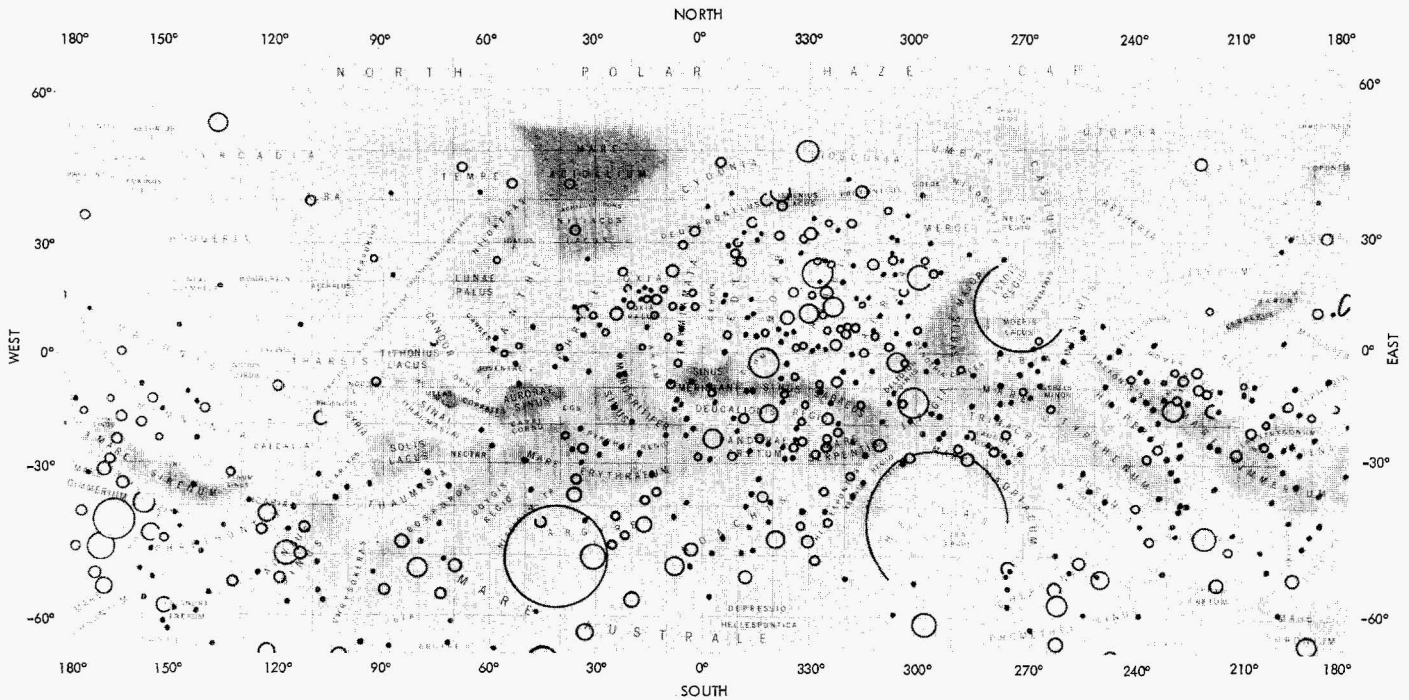
Fig. VIII-4. Distribution of all craters on Mars larger than 64 km in diameter. Solid dots show craters between 64 and 90 km in diameter; open circles show larger craters scaled to their approximate true size.

Polar, Argyre, and Moeris Lacus basins. The hemisphere centered among the volcanoes near Nix Olympica is sparsely cratered. The fact that the south polar region (except for the inner cap itself, latitude > 80°) is heavily cratered and that *Mariner 9* pictures, after north polar haze clearing, revealed a sparsely cratered north polar region strengthens the hemispheric asymmetry seen in Fig. VIII-4.

The rough division of Mars into heavily and sparsely cratered hemispheres occurs along neither latitude meridians nor longitude parallels. Rather the great circle best fitting the division is inclined from about 50°N to 50°S latitude. It is thus extremely difficult to relate such an asymmetry on a rotating planet to external influences, such as nonisotropic meteoroid bombardment. It appears that the crater deficiency in the volcanic region is due to depletion by internally generated processes.

These processes are indicated by the unique geology of the region. The whole bright, sparsely cratered region surrounding Nix Olympica and Tharsis is elevated several kilometers above the mean Martian radius and surrounded by a strong radial pattern of faults. The Coprates canyon lies radial to the domed region. Shield volcanoes reaching an additional few kilometers above this dome lie near its center. The "desert" between the

volcanic shields is characterized on high-resolution (½ to 1 km) pictures by lobate flow-like structures resembling lunar and terrestrial lava flows.

Clearly, strong volcanic and tectonic activity has obliterated the ancient cratered crust in the Tharsis volcanic dome, the Elysium volcanic dome, and nearby areas. The nature of such processes will be discussed elsewhere in a separate paper;[1] evidence points to crustal updoming of a type recognized on Earth and reflecting incipient convection, but falling short of full-fledged plate tectonics as developed on Earth. It is of interest to note that hemispheric asymmetries of crustal structure appear on the Moon (mare/terra), Mars, and Earth (oceanic/continental), probably indicating that primeval uniform surfaces become heterogeneous through the action of impact basin formation, sediment deposition, and mantle activity.

E. Relative Dating: Survey of Crater Densities

Figure VIII-5 shows the map of Mars contoured according to density of craters of $D \gtrsim 64$ km. There is no correlation between the density of these large craters and

---

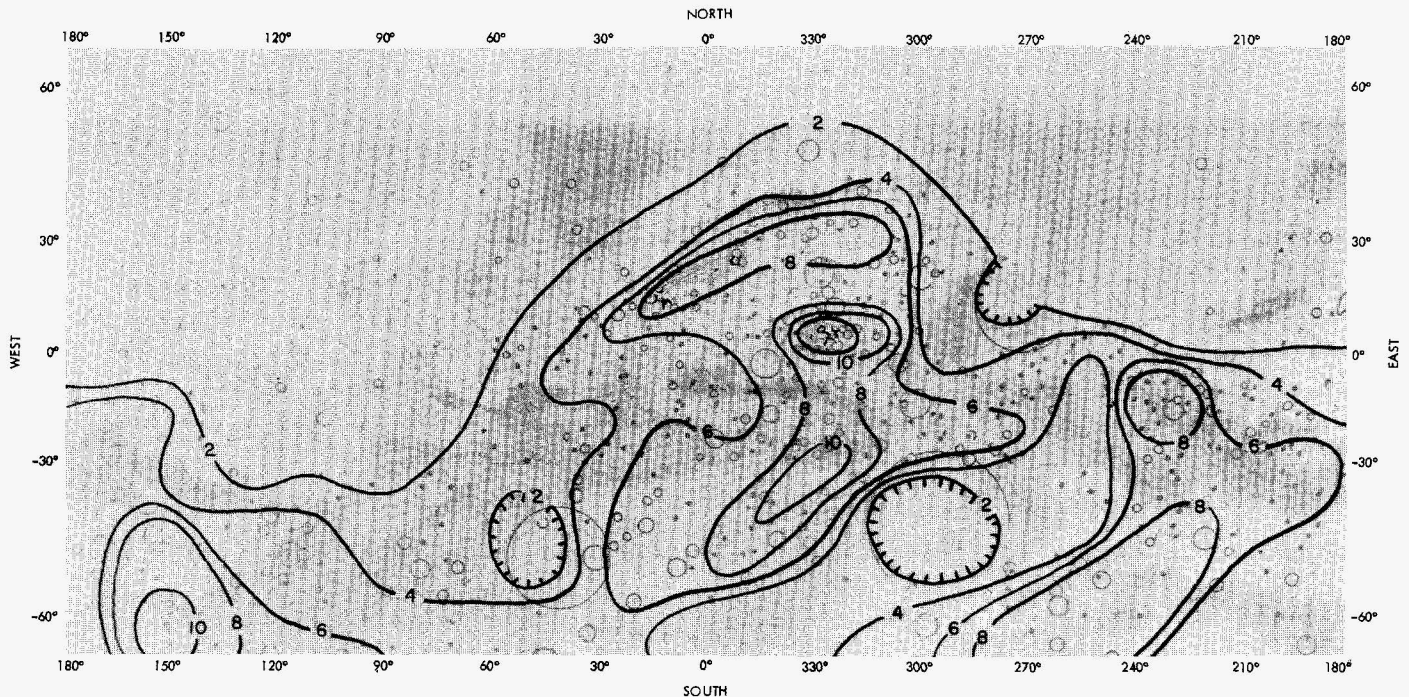[1]Accepted for publication in *Icarus*.

Fig. VIII-5. Contours of crater density on Mars for craters larger than 64 km in diameter. Units give the number of craters per equal-area block (block area = 8.05 × 10⁵ km²).

the classical albedo markings seen from Earth. Although a number of bright "deserts," such as Tharsis, Elysium, Argyre, and Hellas, have much lower density than dark "maria," such as Mare Sirenum and Sinus Sabaeus, a simple correlation between darkness and high crater density is violated by the large, bright cratered regions of Moab and Arabia. Hence, craterform surface irregularities or crater ejecta patterns are not the direct cause of the classical markings.

The largest Martian basins, indicated on Fig. VIII-5, have bright featureless floors where crater density is anomalously low. This suggests either that the basins are being filled in by blowing dust, or that such dust (of light color) has formed a veneer over smooth, stratigraphically young lava deposits similar to those that filled the largest lunar basins.

An examination of Martian crater densities on the global scale, as revealed by Figs. VIII-4 and VIII-5, suffices to construct a generalized stratigraphic column, i.e., a relative chronology, which is shown in Table VIII-1. This part of this section describes this, and subsequent parts indicate the degree to which absolute dates can be determined, and how the varying shape of the crater diameter distribution can be used to interpret localized geologic history.

Figure VIII-6 is a summary of Martian cratering data and serves as a useful introduction to the discussion of erosion history. That the heavily cratered region falls below the saturation line found on the Moon is a sure indication that substantial erosive and depositional processes have destroyed the earliest traces of accretion. However, the high density of craters in regions such as Deucalionis Regio and neighboring areas photographed by *Mariners* 6 and 7 suggests that these areas are quite primitive and may date back to the end of the accretion process. This conclusion is in accord with the previous analyses of Martian cratering, as discussed in the first part of this section. The marked irregularity in slope of the cratering curve for heavily cratered areas at diameters about 5 to 50 km is a strong indication that many smaller craters have been obliterated, as lunar, cometary, and asteroid observational data indicate that the initial diameter distribution of craters smaller than about 64 km should be a power law forming a straight line with slope about -2 (Refs. VIII-11 and VIII-20).

A significant new feature revealed by *Mariner* 9 is the behavior of craters smaller than 4 km in diameter, as shown in Fig. VIII-6. In both the heavily and sparsely cratered regions, this curve displays the approximately -2 slope characteristics of uneroded terrain, where no craters have been removed from the initially produced

Table VIII-1. Preliminary relative chronology based on observed crater densities

Time	Event	Observational data
Recent	Minor erosion and obliteration at sub-hectometer scale (greater rate than lunar erosion)	Dust storms, variable deposits, but lack of severe crater obliteration among hectometer-scale craters ($D < 100$ m)
Episodic?	Flow channel formation (water flow?)	Sparsely cratered, dendritic, sinuous flow channels
Continuing process?	Cyclic deposition and destruction of pre-existing relief in polar caps	Sparsely cratered polar regions (latitude 75° with layered structure)
	Shield volcano formation	Sparsely cratered shields near Tharsis and elsewhere
	Subsidence and collapsing	Fractured and partly destroyed craters around rim of chaotic terrain
Relative chronology uncertain	Extensive volcanism	Flows and large shield volcanoes in sparsely cratered provinces in and around Tharsis
	Stressing and tectonic fracturing	Major lineament pattern radial to elevated Tharsis region
	Transport and partial infilling of major basins, e.g., Hellas	Sparsely cratered, bright floors in depressed basins
	Modest erosion transport, deposition, and crater obliteration	Evidence for partial obliteration (by filling?) of intermediate-size, old craters (10 km $< D <$ 60 km); deficiency of kilometer-scale craters with respect to Phobos
	Extensive erosion	Even most heavily cratered provinces are not quite saturated with craters
	Formation of large basins, e.g., Hellas	Traces of ejecta blanket around Hellas
Very early	Heavy cratering, accretion	Most heavily cratered provinces nearly saturated

diameter distribution. Most of these craters are sharp and bowl-shaped, as first discussed in detail by Murray et al. (Ref. VIII-18). These facts, together with the evidence for heavy early erosion, indicate that the amount of erosion on Mars in the recent geologic past is less than in the distant past. While the average rate of erosion has shown a decline, we cannot be sure that the decline has been monotonic, as the existence of arroyo-like channels and stratified polar deposits strongly suggests episodic variations in erosive rates superimposed on the general decline. While these qualitative interpretations are summarized in Table VIII-1, we will next attempt a more quantitative interpretation.

F. Absolute Dating: Interplanetary Correlations in Cratering Chronology

In analyzing craters on the Martian surface, we are in the favorable situation of having already dated cratered comparison surfaces on two planets, and uneroded surfaces near Mars on Phobos and Deimos. All these surfaces, in different regions of the solar system, can be utilized as control surfaces. The question addressed here is how best to utilize these data in order to illuminate Martian chronology.

It is desirable to prepare a master diagram showing crater density versus age for all dated surfaces in the solar system. From this could be read the ages of Martian provinces on the basis of known crater densities. In principle, such a diagram could be purely empirical although, in the present stage of exploration, some assumptions must be made about the mass distribution of impacting bodies and about time behavior of cratering in the past, as indicated by the following discussion.

Let D = crater diameter, T = crater retention age of surface for specified D, F = crater frequency for the same specified D (also called crater density), and R = rate of formation of craters/km² for craters of the same specified D. If the cratering rate, R, were constant

$$T = F/R$$

But we know from *Apollo* and *Luna* analyses that R has not been constant. Therefore, we assume only that the time dependency of the cratering rate, $R(t)$, has been the same for all planets, i.e., normalizing to the Moon

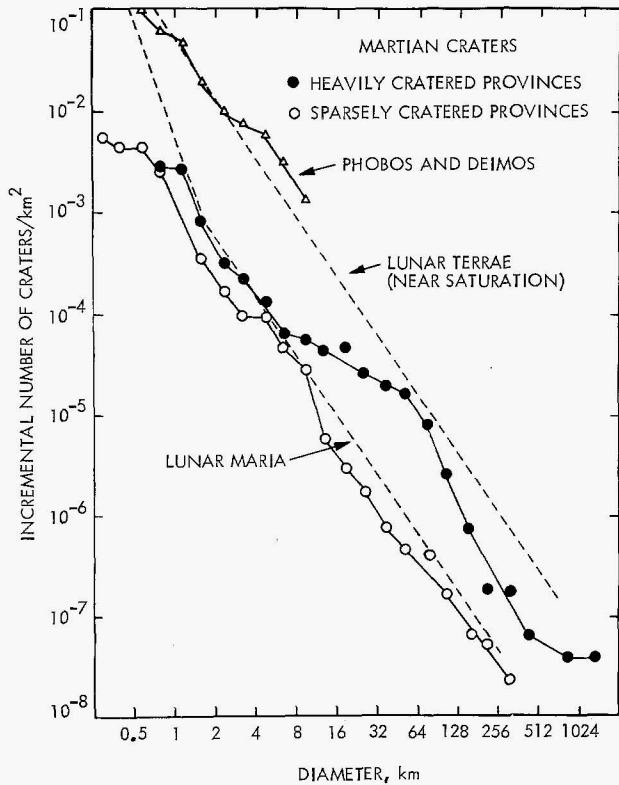$$R(t)_{planet}/R(t)_{Moon} = k_{planet} = \text{constant for all times } t$$

Fig. VIII-6. Diameter distributions of craters (averaged from many *Mariner 9* pictures) in heavily and sparsely cratered Martian provinces (defined in text). For comparison, the uppermost curve (triangles) shows crater densities observed on Phobos and Deimos. Martian craters smaller than 8 km are deficient by one to two orders of magnitude relative to Phobos and Deimos, a fact indicating extensive Martian crater obliteration processes.

Thus, k varies from planet to planet, but for any planet is time-independent. In terms of accretionary theory of planet growth, this is equivalent to assuming that the solar nebula cleared uniformly, although the density of interplanetary debris depended on position.

The crater retention age of a surface on any planet should therefore be proportional to a quantity defined here as adjusted crater density, F/k; that is

$$T = F/R_{planet} = F/kR_{Moon} \propto F/k$$

The objective of this discussion is thus to construct an empirical plot of *adjusted crater density, F_{planet}/k*, against age for dated surfaces, so that data from all planets will fall on a single curve, which may then be used to date Martian surfaces.

Cratering rate is defined here as the rate of formation of craters of a specified D, or as the rate of impacts of

given energy, but not as the number of impacts by particles of a given mass. The difference arises because the impact velocity on different planets differs because of orbital and gravitational effects. Modal impact velocities for the Moon, Mars, and Earth are listed by various sources as 14, 10, and 18 km/sec, respectively (see summary by Hartmann in Refs. VIII-8 and VIII-19). According to energy scaling laws, crater diameter is approximately proportional to $(MV^2)^{1/3.3}$, where M = meteorite mass and V = velocity. Hence, to match a lunar crater of given size requires a terrestrial impact by a meteorite only $0.6\times$ as massive as that striking the Moon and a Martian impact by a meteorite $2\times$ as massive.

We will now attempt to define the relative Martian, terrestrial, and lunar cratering rates (i.e., k values) by normalizing to the Moon because the best crater statistics and related age data are lunar. Determination of k requires determination of the space density of meteoroids at the planetary orbit, determination of gravitational cross-section effects, and determination of impact velocity effects. In the case of Earth and the Moon, the main difference in k is caused by gravitational cross-section differences, as pointed out by Mutch (Ref. VIII-27), who derives a terrestrial impact rate $2.15\times$ as great as the lunar rate for a given mass. Because terrestrial meteorites strike at higher velocity, bodies only $0.6\times$ as massive are required to cause a crater of the same size as a crater formed on the Moon. Hence, because of the meteoritic mass distribution law for cumulative number, N, and mass, M, $N \propto M^{-0.7}$, this corresponds to an increase by 1.4 in cratering rate, giving 1.4×2.15, i.e., a rate $3.0\times$ higher on Earth than on the Moon. However, this must be reduced by several factors, such as the focusing effect of the Earth on the front face of the Moon and the size-dependent atmosphere breakup of weak meteoritic and cometary material in Earth's atmosphere. These factors are discussed in more detail by Hartmann in Ref. VIII-8. It is thus concluded that the effective terrestrial crater formation rate is about $2\times$ higher than that on the Moon for the crater sizes considered here (1 to 100 km).

To determine the cratering rate ratio, k, for Mars, we must first investigate the meteoritic environment at Mars. Four sources of data serve to estimate the Martian meteoritic environment: (1) The *Mariner 4* dust detector measured a micrometeorite flux (impacts m^{-2} sec^{-1}) increasing away from Earth to a value of $4.5\times$ that at Earth, measured at the perihelion of Mars. Beyond perihelion, lower values were recorded, suggesting that Mars efficiently sweeps up material in orbits overlapped by its own. The mass distribution recorded for small

particles near Mars orbit was similar to that near Earth (Ref. VIII-28). (2) Dycus (Ref. VIII-29) has reviewed meteorite distribution in the solar system and concluded that the flux in undisturbed space at Mars averages $14\times$ that at Earth's orbit, and at the top of the Martian atmosphere, $7\times$ that at the top of Earth's atmosphere. (3) Data of Anders and Arnold (Ref. VIII-5), from a computer calculation of asteroid histories, give an asteroidal flux at Mars about $25\times$ the meteorite flux at Earth. (4) Data on known Mars-crossing asteroids and their lifetimes have been utilized by the author, along with data of Öpik (Ref. VIII-30) and Dycus (Ref. VIII-29), to compute Martian environment fluxes for the largest impacting bodies. All these data taken together are relatively consistent in agreeing on the following statement: The particles in Mars' orbit have the same mass distribution as that measured near Earth and the Moon, but have about one order of magnitude higher number density, with an uncertainty of about a factor of 3. Because these particles impact Mars at 10/14 the speed that applied to impacts on the Moon, particles $1.96\times$ larger are needed to form a crater of given size; hence, the cratering rate is diminished by $1.96^{-0.7}$, or 0.62. Hence, the Martian cratering rate is $6.2\times$ the lunar rate.

The uncertainty of a factor of 3 in Martian flux immediately indicates that our absolute dates will have an uncertainty at least this large. However, our current total ignorance of absolute Martian chronology makes the ability to discriminate even 10^7 and 10^9 year old surfaces useful.

In order to plot the desired diagram of adjusted crater density, D/K versus age, it is necessary to summarize available data on dated cratered surfaces in the solar system. Lunar data through *Apollo 15*, including *Luna 16*, have been analyzed in detail by Hartmann (Ref. VIII-31). Astroblemes on the Canadian Shield, which has an exposure age of about 1.3 aeons and is younger than the lunar surface, were analyzed by Hartmann (Ref. VIII-32) and Baldwin (Ref. VIII-33). Fifteen astroblemes larger than $D = 8$ km were cataloged in an area of 3.7×10^6 km². In order to extend our time scale, it is desirable to find a considerably younger area that is cratered and well studied; for this reason, certain eastern states in the United States, covered with Paleozoic and Cenozoic sediments of exposure age about 0.3 aeon, were studied. This updates an early analysis by Shoemaker et al. (Ref. VIII-34). Ten astroblemes or crypto-volcanic structures of $D > 4$ km were cataloged in a ten-state area of 1.72×10^6 km².

In the lunar areas cited, the diameter distribution of craters, and hence the crater density F, is well defined, and most of the relevant crater counts have been published. However, in the Canadian Shield and eastern United States, erosion effects are important, and a detailed discussion is in order.

Diameter distributions of craters in Canada and in the eastern United States are plotted in Fig. VIII-7. The distributions probably do not follow the normal -2 power law by craters on well preserved surfaces, as expected in view of the active erosion in the regions considered. The effective exposure ages of the two areas are estimated to be 1.1 and 0.3 aeons, respectively. In order to measure the crater density in these eroded terrestrial provinces, from the scanty statistical sample, we assume the basic premises of Hartmann (Ref. VIII-20), to which the reader is referred. The result of that discussion is that, at sufficiently large diameter, the original -2 power law will be followed, whereas below a certain diameter, erosion will have affected the distribution, and a more gentle (less negative) slope or a turnover will be observed. Under certain idealized circumstances of extended obliteration by deposition, a -1 power law is expected, but a sharp episode of deposition would produce a sharp cutoff. According to the 1971 discussion (Fig. VIII-2), the smallest diameter crater retained since province formation in the Canadian province (1.1 aeon) is about 128 km and in the U.S. province (0.3 aeon) is about 32 km. Therefore, in order to deduce the crater density from Fig. VIII-7, we have several useful boundary conditions:

(1) Slopes of about -2 are expected above the diameters mentioned.

(2) Immediately below the diameters mentioned, a more gentle slope is expected.

(3) Numbers of astroblemes known in the literature are sufficiently large to give some confidence that the intercepts (vertical positions) of these curves can be located in Fig. VIII-1.

(4) Crater density (intercept) in the Canadian Shield should be higher by a factor of 3.7 than that in the eastern United States because of its greater exposure age.

Figure VIII-7 includes dashed curves that show the interpreted North American crater densities based on the above considerations. The similarity of the data in the segments with -1 slopes indicates similar obliteration rates, i.e., similar extended erosion effects, in the Canadian and U.S. provinces.
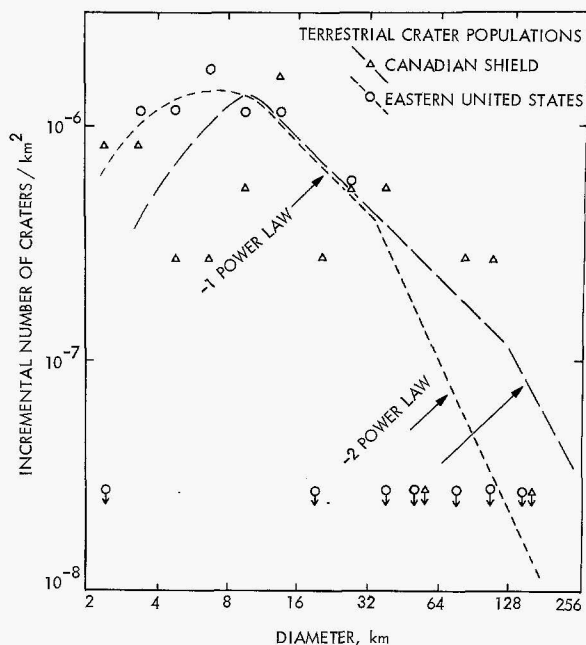
Fig. VIII-7. Attempts to derive crater densities on the Canadian Shield and in the eastern United States. Intervals containing no craters are shown by downward pointing arrows at the bottom. The dashed lines are fitted to the data following theoretical boundary conditions (described in text).

In order to compare crater densities on different planetary surfaces, we must now adopt a convention for expressing crater density. This could be done, for example, by using the cumulative number of craters/km² larger than a certain size; for example, 64 km or 1 km. But a

difficulty arises because, at 1 km, erosive effects are large on Earth, and confusion with secondary craters and endogenic craters exists on the Moon. If we adopt a diameter cutoff as large as 64 km, which would avoid the terrestrial erosion problem, we are limited to large areas with consequent low resolution of specific dated geologic provinces. Clearly, some intermediate diameter is optimum and some extrapolation and interpretation of crater curves will be necessary, as was exemplified by the *extreme* case of interpretation required in Fig. VIII-1. I have previously adopted a convention that seems to remain useful here. Instead of defining crater density in terms of actual cumulative numbers per kilometer at a certain diameter cutoff, a relative crater density scale is used, the average overall front-side lunar maria defined as unity, as this provides the best combination of crater statistics and age determination of any solar system surface. The maria present, incidentally, a cumulative crater density of $F = 2.0 \times 10^{-4}$ craters larger than 4 km/km². Densities on other stratigraphic units are determined by comparing the entire diameter distribution, with emphasis given to the diameter range from 2 to 64 km (where statistics are good), with no weight given to diameter ranges where the slope seriously departs from values between -1.8 and -2.2 (a departure in all cases so far studied believed to result from erosion processes).

Table VIII-2 shows the data we have assembled and allows a plot correlating ages and crater densities on various planets. Figure VIII-8 shows this plot. The dashed line in Fig. VIII-8 shows that the data for the

Table VIII-2. Crater data for dated[a] surfaces

Surface	Age, aeons	Crater density, D, relative to lunar material	Applicable relative cratering rate, k	Adjusted crater density, D/k
Moon, Uplands	4.4?	>32 (saturated)	1	32
Phobos, Deimos	4.2?	>32 (saturated)	6	5.4
Apennine Front	4.1	2.9	1	2.9
Fra Mauro	3.9	2.5	1	2.5
Mare Tranquillitatis	3.6	1.6	1	1.6
Mare Fecunditatis	3.45	0.6	1	0.6
Palus Putredinis	3.3	0.35	1	0.35
Oceanus Procellarum	3.2	0.75	1	0.75
Canadian Shield	1.3	0.67	2	0.33
Eastern U. S.	0.3	0.13	2	0.065

[a]For saturated surfaces such as the lunar uplands, Phobos, and Deimos, there are no radioisotopic dates, but the saturation with craters and independent calculations of cratering rates during early accretion history suggest ages near that of the solar system.
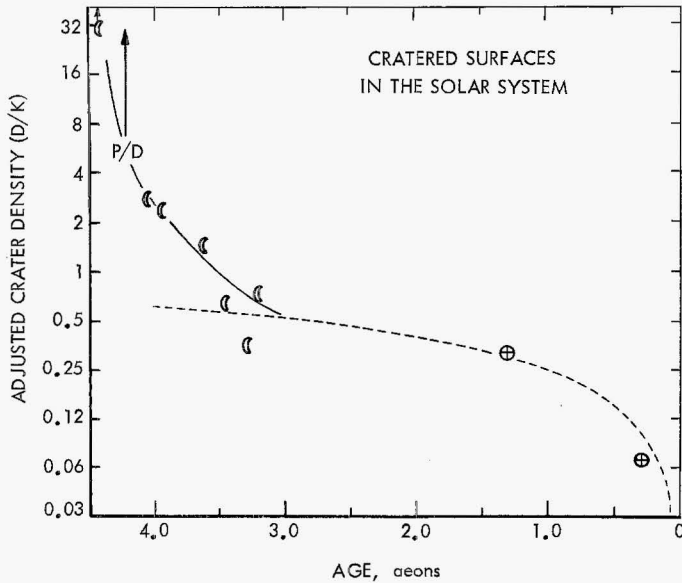
Fig. VIII-8. Synthesis of solar system data on age of cratered dated surfaces on Earth and the Moon. P/D marks assumed age and measured crater density on Phobos and Deimos. Age is plotted versus "adjusted crater density" as defined in text. Dashed line shows a fit assuming constant cratering rate; before 3 aeons, the cratering rate was much higher. Estimated ages of Martian surfaces are read as discussed in text.

last 3 aeons are compatible with a constant cratering rate, within a factor of 2; but before 3 aeons ago, the cratering rate was much higher. This result has been found previously by Öpik (Ref. VIII-9), Hartmann (Refs. VIII-19 and VIII-32), and Baldwin (Ref. VIII-33). The constancy of the cratering rate in the last 3 aeons gives added confidence that we can date young Martian features, such as Nix Olympica, by direct scaling to known cratering rates measured on Earth and the Moon, without much concern for our assumption that the time behavior of change in cratering rate was the same for Mars, Earth, and Moon.

G. Absolute Dating: Analysis of Erosion History

Figure VIII-9 shows an application of cratering theory to the raw data used in Fig. VIII-6. Several theoretical curves are given to indicate the predicted crater diameter distribution at various times in the past, under conditions hypothesized for Mars. These theoretical curves, to be discussed below, are based on the crater obliteration theory developed in various forms independently by Öpik (Ref. VIII-9), Hartmann (Refs. VIII-8 and VIII-20), and Chapman et al. (Ref. VIII-11). The specific theory applied here was first developed in essentially the pres-

ent form in an unpublished thesis by Chapman (Ref. VIII-35).

The theoretical curves in Fig. VIII-9 are developed as follows: From the previous paragraphs, we have a best estimate of the crater formation rate on Mars at present. This is $6.2\times$ the lunar rate, or 3.54 (10^{-4}) craters larger than 4 km/km²/aeon. Thus, curves AA' and BB' in Fig. VIII-9 can obviously be constructed to represent the numbers of craters formed in 10^8 years and 10^9 years, respectively, at the *present* cratering rate. The number of craters formed in 4×10^9 years (CC') is not so easily plotted, however, as the early cratering rate is believed to have been nonuniform. Curve CC', therefore, is based on the data in Fig. VIII-8 and lies at $9\times$ curve BB' ($\neq 4\times$ curve BB'). Curves AA', BB', and CC' all reflect cratering with no erosion whatsoever.

Curve EE' represents the steady state of craters under a constant rate of deposition, about 10^{-4} cm/yr in crater
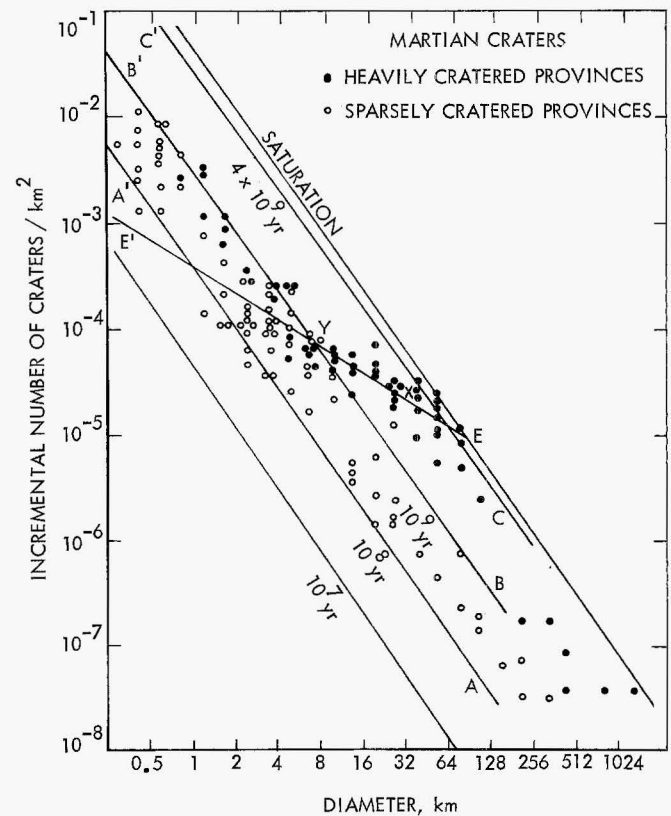

Fig. VIII-9. Raw crater counts for heavily cratered and sparsely cratered provinces on Mars (compare averaged results in Fig. VIII-6), with theoretical isochrons as derived in text. Solid lines marked 10^7, 10^8, 10^9, and 4×10^{11} years show crater densities expected with no erosion for surfaces of the indicated ages. The line EE' is a theoretical result based on erosion and deposition at a constant rate (see text).

floors. This deposition can be viewed as principally due to windblown dust, as discussed by Hartmann in Ref. VIII-20, or as a cumulative effect of various other erosion processes of constant effect averaged over long periods. (Deposition at other constant rates would have the same slopes, but different vertical intercepts. Deposition at non-constant rates would have different slopes. Sudden catastrophic deposition, e.g., by lava inundation, would produce a near-vertical cutoff in craters. See works cited above.)

If the heavily cratered regions filled curve CXE', the interpretation would be that these regions formed 4 aeons ago, have been cratered continually since, and have experienced a constant erosion and deposition rate with 10^{-4} cm/yr accumulating in crater floors. However, the heavily cratered regions do not fit the segment XE', but rather have the additional complexity of bending nearly along XYB'. The segment YB' falls on the curve of a surface cratered with no erosion for about the last aeon. It is concluded that:

(1) The oldest parts of Mars reveal a history that begins just after the accretion phase ceased.

(2) The original accreted surface was largely destroyed by early intense erosion (effects of an early dense atmosphere?), accounting for the fact that the surface is not now saturated.

(3) A long period ensued in which erosion occurred at a relatively constant, intermediate rate. (Episodic "fine structure" in this erosion cannot be excluded.)

(4) During roughly the last aeon, the erosion and deposition rate has been so much reduced from its former value that most kilometer-scale craters this young show negligible erosion effects.

In Ref. VIII-20, the bowl-like morphology of kilometer-scale craters, noted by Murray et al. (Ref. VIII-18), was treated as an unsolved puzzle. This is now accounted for by the lack of recent erosion. Indeed, it is now clear that the sharp, bowl-like morphology and the complete preservation of these craters reflected in the diameter distribution strongly *necessitate* the conclusion that erosion on Mars recently has been much reduced from its former values.

Figures VIII-10 and VIII-11 present the detailed curve fitting, based on the idealized, simple theory presented above, for the raw data applying to the heavily and sparsely cratered regions, respectively. The theoretical curve fitted to the heavily cratered provinces (Fig.
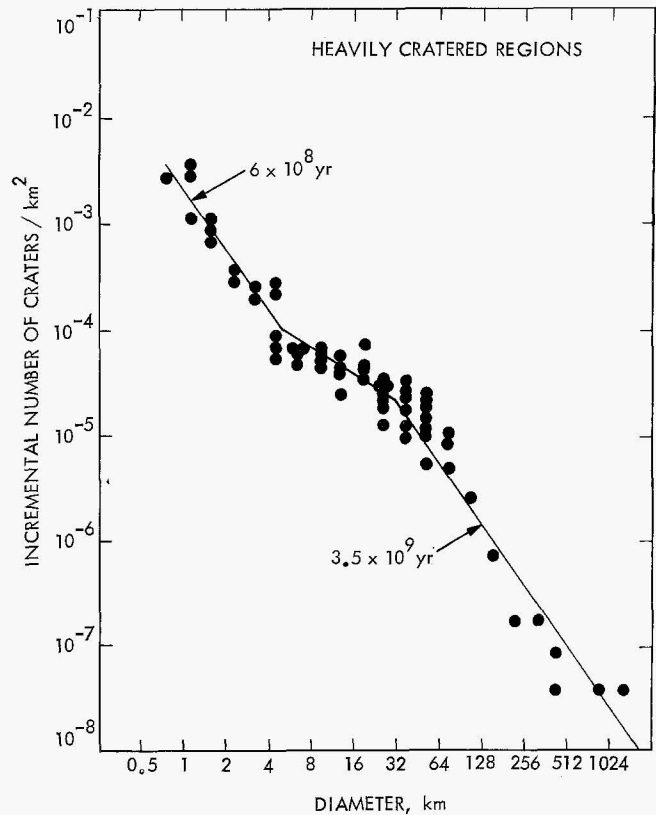

Fig. VIII-10. Crater diameter distribution in heavily cratered regions fitted to two isochrons (3.5 and 0.6 aeons) and showing a flattened segment characteristic of deposition before 6 aeons ago.

VIII-10) would fit a 3.5-aeon-old region in which deposition in craters occurred at a rate of 10^{-4} cm/yr until 0.6 aeon ago. The fitted curve assumes that erosion was negligible for the last 0.6 aeon. The curve fitted to the sparsely cratered region describes an area that formed (by volcanic inundation?) 0.3 aeon ago. A marginal "kink" in the curve between 2 and 4 km suggests some erosion (perhaps the end of the erosion indicated by Fig. VIII-10?) reduced to a negligible value by 0.25 aeon ago.

Figures VIII-10 and VIII-11 contain data summarizing the two dissimilar hemispheres of Mars. Their analysis, in the preceding paragraph, is believed to indicate in first-order terms the erosional history of Mars. In detail, the history may be more complex. The essence of the conclusion supports an inference by Binder and Cruikshank (Ref. VIII-36) that a much more extensive atmosphere was required in the past to create the limonite, or oxidized basalt, coloring Mars, and at the same time sheds light on the existence of arroyo-like channels. The implication is that a denser atmosphere and greater
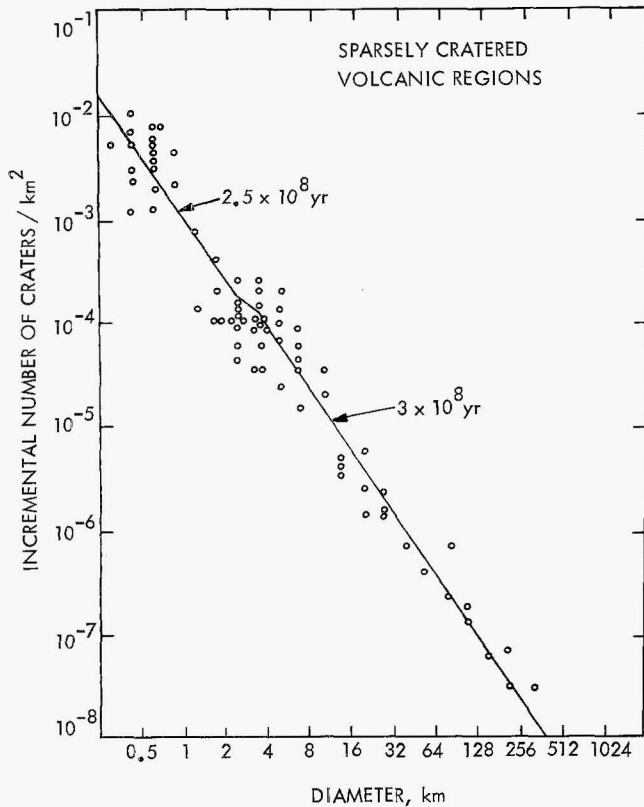
Fig. VIII-11. Crater diameter distribution in the sparsely cratered, volcanic regions fitted to isochrons from Fig. VIII-9. The flattened segment between 3 and 2.5 × 10⁸ years is of marginal significance, but serves to illustrate resolution in time scale.

humidity applied before 600 million years ago on Mars, and that only the volcanic provinces, such as Tharsis, exhibit surfaces contemporaneous with the post-Cambrian stratigraphic column on Earth.

H. Absolute Dating: Martian Shield Volcanoes

Figures VIII-12 through VIII-15 show attempts at detailed analysis of specific Martian features, namely four of the widely publicized volcanoes with summit calderas. These were chosen as probable representatives of the youngest constructional geologic features, whose dating would indicate the most recent volcanic activity of major extent on Mars.

The principal problem here is the abundance of volcanic pit and chain craters that lie on the flanks of the large volcanoes. By counting all discernible craters (as has been done in the preceding paragraphs, with the exception of the large obvious calderas such as Nix Olympica), one would count many endogenic craters along with impacts and determine only an upper limit
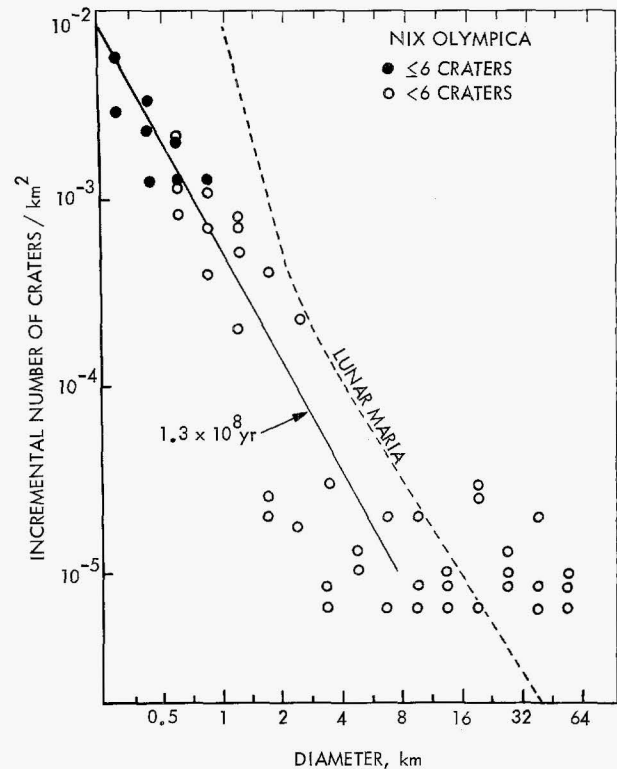

Fig. VIII-12. Crater diameter distribution observed on slopes of Nix Olympica volcano with that from lunar maria for comparison. Craters larger than 8 km in diameter are primarily calderas near the summit. Solid line is an isochron corresponding to primary impact cratering for 1.3 × 10⁸ years.

on age. In the case of Nix Olympica (Fig. VIII-12), clearcut calderas of $D > 16$ km cluster near the summit, but the craters of $D < 2$ km on the slopes define a fairly clear curve with slope equal to that expected for the impacts. Thus, the low-diameter end is used to fit an isochron as shown in Fig. VIII-9, and this curve is found to correspond to an age about 1×10^8 years. A different technique is used for the volcanoes near Nodus Gordii (Fig. VIII-13) and Ascraeus Lacus (Fig. VIII-14). All craters were counted, but then suspected impacts were separated out by rim and interior morphology and plotted with a different symbol. The isochrons fitted were weighted toward the data for impacts only. In Fig. VIII-14, the additional measure was taken of counting craters on the floor of the plain immediately in contact with the base of the Ascraeus Lacus shield. It was found that the sum of all craters outnumbers the craters on the plain, indicating once again that the shield has an admixture of endogenic craters, since the shield is assumed to have a constructional surface younger than the plain. The counts of probable impacts fit fairly well with the counts of craters on the plain, which is believed to
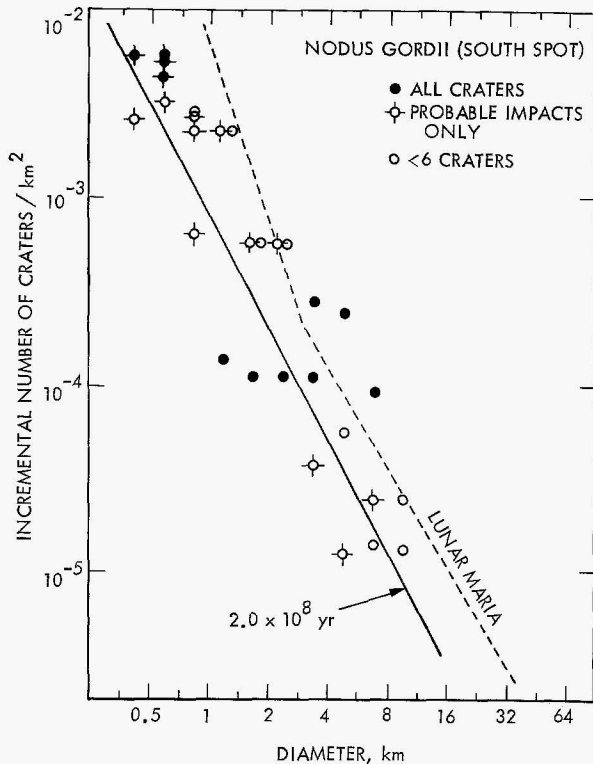
Fig. VIII-13. Crater diameter distribution for Nodus Gordii volcano, with comparison to lunar maria. Solid line is an isochron fitted to probable impact craters only and indicates primary impact cratering for 2×10^8 years.
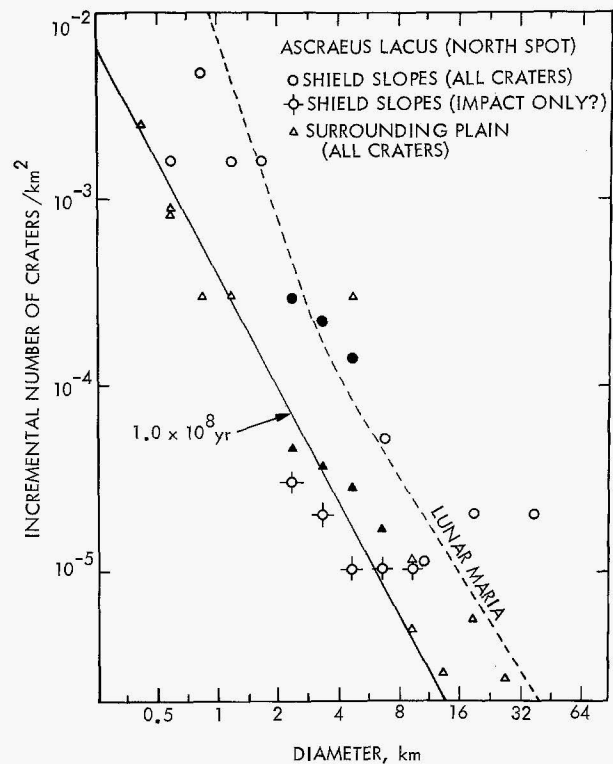

Fig. VIII-14. Crater diameter distribution on Ascraeus Lacus volcano with comparison to lunar maria. Solid line is an isochron fitted to probable impact craters and indicates primary impact cratering for 1×10^8 years. Solid data points = 6 or more craters/diameter increment in each picture studied; open circles, less than 6.

be relatively free of endogenic craters. For Pavonis Lacus (Fig. VIII-15) the craters counted were, on most of the pictures, not readily distinguishable into impact and non-impact craters, but it was believed, on the basis of fault patterns, that some of the smaller craters may associate with chains and clusters of endogenic craters. Thus, the drawn isochron is weighted toward the less abundant larger craters ($D > 2$ km).

An upper limit of age can be based on isochrons drawn through the data for all craters, although it is believed that the isochrons in Figures VIII-12 through VIII-15 are closer to the actual caldera ages. It is concluded in this way that all four of the well known volcanoes have surfaces that formed less than 500 million years ago. Within the uncertainty of the method, they all appear to have formed about 100 million years ago.

I. Absolute Dating: South Pole

It is evident from *Mariner 9* pictures that, in the extreme polar zones, craters have been obliterated and replaced by topography composed of numerous stratified

layers. Original relief must have been destroyed, as there is no mechanism to prevent craters from forming at the poles. The fall-off in crater density is particularly sharp between 80° and 81°S latitude.

Mariner 6 and *7* results indicated a lower crater density near the south pole than elsewhere (Ref. VIII-20), but it remains of interest to estimate the age of the youngest regions as an indication of the youth of recent erosion and deposition processes on Mars. The following paragraphs present a preliminary analysis of the extreme south polar region south of 81° latitude, based on the data in Fig. VIII-16.

Because of the sparseness of cratering and the small size of the region considered, the statistics on craters are scanty. The few large craters present ($D > 8$ km) have been recorded on the USGS airbrush south polar map; in addition, counts have been made on several wide- and narrow-angle pictures of *Mariner 9* and two *Mariner 7* pictures. In view of the paucity of craters, it
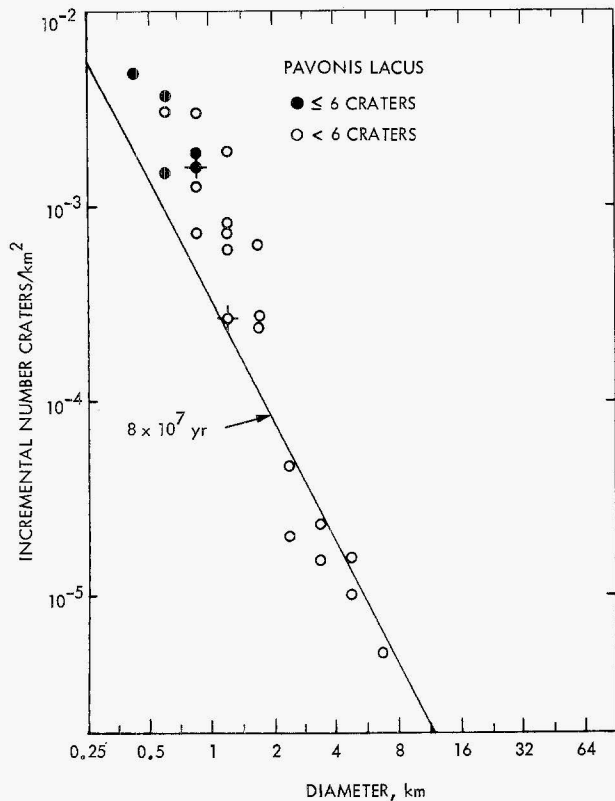
Fig. VIII-15. Diameter distribution of craters on Pavonis Lacus volcano. Solid line is an isochron indicating primary impact cratering for 8 × 10⁷ years.
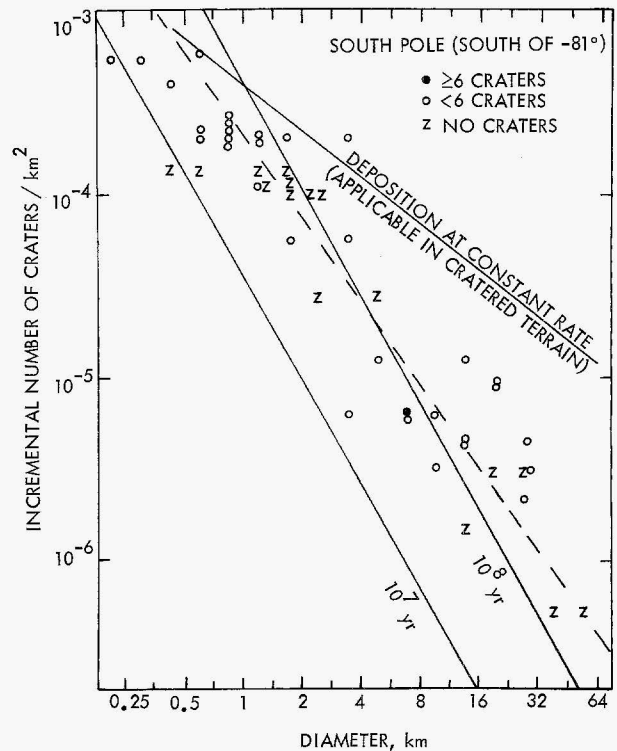

Fig. VIII-16. Diameter distribution of craters through extreme south polar region (south of −81°). Isochrons of 10⁷ and 10⁸ years are indicated, but these have steeper slopes than the dashed line which is fitted to the observed data. The data are interpreted to indicate deposition at a declining rate; 1-km craters in the south polar zone appear to be less than 10⁸ years old. "Z" indicates diameter increments with no craters counted on each picture studied (see text for method of plotting).

was believed helpful to indicate diameter increments on Fig. VIII-16 where no craters were counted on some pictures. These instances are represented as Z points and are plotted in Fig. VIII-16 at a vertical position corresponding to one-half crater. This was done up to 2 diameter increments beyond the largest observed crater in a given picture and in "empty" diameter increments bracketed by increments with craters. Only one picture in this region yielded as many as six craters in a single diameter interval. The counts at $D > 1$ km are regarded as defining the upper limit of impact crater density in the polar zone, since I attempted to include all possible craters, including degraded examples, except for irregular depressions in the "pitted terrain" (deflation basins?). However, for $D < 1$ km, it is conceivable that incompleteness is more important than in Figs. VIII-12 through VIII-15, as the polar pictures were taken at ranges usually exceeding 3000 km, while the volcanoes were photographed frequently from less than 2000 km.

As seen in Fig. VIII-16, the data points from the sparsely cratered pole cluster around the isochron for about 1×10^8 years. However, it can be seen that the

dashed line, of slope −1.6, is a better fit than the isochron of −2 slope. A curve of −1.6 slope does not fit the model of obliteration by deposition at a constant rate (slope −1), which has been referred to and applied above (e.g., Figs. VIII-9 and VIII-10). However, as pointed out by Chapman (Ref. VIII-35), a curve of slope intermediate between −2 and −1 fits a situation with erosion/deposition *declining* at a constant rate. As it does not appear that incompleteness in counts of small craters can be sufficient to create the observed shallow slope, it is concluded that the slope is closer to −1.6 than to −2.

Considering the previous data on other regions of Mars, the most straightforward interpretation of the polar data is that erosion and/or deposition rates were much greater in the past at the pole and in other parts of Mars than they are now. While these processes terminated or declined abruptly in other parts of Mars about 6×10^8 years ago, they declined more slowly in

the polar zone. Deposition in stratified layers, possibly by trapping of dust in seasonal and perihelic dust storm cycles, continues at a decreasing rate today, and this rate is higher near the poles than on the volcanic shields studied here. Crater retention ages (lifetimes) at the south pole may be approximately 3×10^6 years for 32-km craters, and only 6×10^7 years for 1-km craters.

J. Summary and Conclusions

Early analyses of cratering and other Martian surface properties that indicated extensive ancient erosion have been strongly supported by *Mariner 9* data. Positive evidence of erosive loss of Martian craters comes from the much greater abundance of kilometer-scale craters on Phobos and Deimos than on the Martian surface (Fig. VIII-6). Craters of various classes of complexity are found on Mars as well as on Earth and the Moon. By their great variations in density, these craters indicate a history of Martian erosion and crustal development intermediate between Earth and the Moon. Approximately one hemisphere of Mars reveals an ancient cratered surface with craters in varying states of freshness. The diameter distribution does not match the initial production curve, but approximates that predicted by an idealized model of obliteration through deposition of material in craters at a constant rate. In both hemispheres, however, the small craters are sharp, bowl-shaped, and match the shape of the initial production curve. This indicates strongly that, in the recent past, the erosion and deposition declined markedly, so that recent craters have been preserved in nearly their original form.

The volcanic region around Tharsis was fractured and resurfaced by lava flows near the time of, or more recently than, the termination of the erosion. Craters in this region are generally well preserved, and the shield volcanoes near Nix Olympica, Nodus Gordii, Ascraeus Lacus, and Pavonis Lacus are among the youngest, large-scale constructional features. The sparsely cratered area within 9° of the south pole has an age similar to that of the shield volcanoes.

I have attempted to go beyond the relative chronology to establish absolute dates for some of the events mentioned. The major source of uncertainty is in the rate of impacts on Mars, resulting in an uncertainty of at least a factor of 3. Within these limits, it is believed that the oldest surfaces, such as that near Deucalionis Regio, display craters dating back 3 to 4 aeons ago (Fig. VIII-10), but not back to planet formation, since the region is not saturated with large craters as is the lunar terrae. From that time until about 6×10^8 years ago, erosion and deposition were much more extensive than they are now, and an effective deposition rate in craters is estimated at 10^{-4} cm/yr applied during much of this period. It is surmised that much dust accumulated during this period in the now near-featureless basins of Hellas and Argyre. About 6×10^8 years ago, the erosion rate declined quite rapidly in most regions, but perhaps less rapidly in the polar regions (Fig. VIII-16). The sparsely cratered regions around Tharsis were resurfaced about 3×10^8 years ago by volcanic activity (Fig. VIII-11), which produced the four major shield volcanoes about 1×10^8 years ago (Figs. VIII-12 through VIII-15). Deposition declined more slowly at the poles, adding to the stratified deposits and causing the diameter distribution to have a diagnostic intermediate slope. Lifetimes of kilometer-scale craters near the pole may be as low as 6×10^7 years.

There is no strong evidence in the cratering data for episodic erosive events. Catastrophic episodes of erosion can be ruled out, since they would produce characteristic downward bends (positive slopes) or sharp cutoffs in the diameter distribution, and these are not observed. Minor erosion episodes such as discussed by McGill and Wise (Ref. VIII-21), possibly even associated with fluvial activity in the sinuous channels, are not precluded, as some channels appear to cut sparsely cratered areas. However, it is suggested that this activity may be a remnant of even more extensive erosion activity in the middle periods of Martian history. The cause and chronology of fluvial activity remains perhaps the most important problem in the Martian studies.

References

VIII-1. Öpik, E. J., "Mars and the Asteroids," *Irish Astron. J.*, Vol. 1, p. 22, 1950.

VIII-2. American Astronomers Report, reference to C. W. Tombaugh, *Sky and Telescope*, Vol. 9, p. 272, 1950.

VIII-3. Leighton, R., Murray, B., Sharp, R., Allen, J., and Sloan, R., "Mariner IV Photography of Mars: Initial Results," *Science*, Vol. 149, p. 627, 1965

VIII-4. Witting, J., Narin, F., and Stone, C., "Mars: Age of Its Craters," *Science* Vol. 149, p. 1496, 1965.

VIII-5. Anders, E., and Arnold, J. R., "Age of Craters on Mars," *Science*, Vol. 149, p. 1494, 1965.

VIII-6. Baldwin, R. B., "Mars: An Estimate of the Age of Its Surface," *Science*, Vol. 149, p. 1496, 1965.

VIII-7. Binder, A. B., "Mariner IV: Analysis of Preliminary Photographs," *Science*, Vol. 152, p. 1053, 1966.

VIII-8. Hartmann, W. K., "Martian Cratering," *Icarus*, Vol. 5, p. 565, 1966.

VIII-9. Öpik, E. J., "The Martian Surface," *Science*, Vol. 153, p. 255, 1966.

VIII-10. Marcus, A. H., "Martian Craters: Number Density," *Science*, Vol. 160, p. 1333, 1968.

VIII-11. Chapman, C., Pollack, J., and Sagan, C., *An Analysis of the Mariner-4 Photography of Mars*, Smithsonian Astrophys. Obs. Special Report No. 268, 1968.

VIII-12. Chapman, C., Pollack, J., and Sagan, C. "An Analysis of the Mariner-4 Cratering Statistics," *Astron. J.*, Vol. 74, p. 1039, 1969.

VIII-13. Binder, A. B., "Martian Craters: Comparison of Statistical Counts," *Science*, Vol. 164, p. 297, 1969.

VIII-14. Leighton, R., Murray, B., Sharp, R., Allen, J., and Sloan, R., "Mariner IV Pictures of Mars," *Mariner Mars 1964 Project Report: Television Experiment Part I: Investigator Reports*, Technical Report 32-884, Jet Propulsion Laboratory, Pasadena, 1967.

VIII-15. Wells, R. A., and Fielder, G., "Martian and Lunar Craters," *Science*, Vol. 155, p. 354, 1967.

VIII-16. Russell, J. A., and Mayo, M., "The Frequency-Size Distribution of Martian Oases," *Publ. Astron. Soc. Pacific*, Vol. 82, p. 138, 1970.

VIII-17. Leighton, R. B., Horowitz, N. H., Murray, B. C., Sharp, R. P., Herriman, A. H., Young, A. T., Smith, B. A., Davies, M. E., and Leovy, C. B., "Mariner 6 and 7 Television Pictures: Preliminary Analysis," *Science*, Vol. 166, p. 49, 1969.

VIII-18. Murray, B. C., Soderblom, L. A., Sharp, R. P., and Cutts, J. A., "The Surface of Mars: 1. Cratered Terrains," *J. Geophys. Res.*, Vol. 76, p. 313, 1971.

VIII-19. Hartmann, W. K., "Martian Cratering II: Asteroid Impact History," *Icarus*, Vol. 15, p. 396, 1971.

References (contd)

VIII-20. Hartmann, W. K., "Martian Cratering III: Theory of Crater Obliteration," *Icarus*, Vol. 15, p. 410, 1971.

VIII-21. McGill, G. E., and Wise, D. U., "Regional Variations in Degradation and Density of Martian Craters," *J. Geophys. Res.*, Vol. 77, p. 2433, 1972.

VIII-22. Oberbeck, V., and Aoyagi, M., "Martian Doublet Craters," *J. Geophys. Res.*, Vol. 77, p. 2419, 1972.

VIII-23. Dence, M., Innes, M., and Robertson, P., "Recent Geological and Geophysical Studies of Canadian Craters," *Shock Metamorphism of Natural Materials*, edited by B. French and N. Short, Mono Book Co. Baltimore, 1968.

VIII-24. Hartmann, W. K., "Interplanet Variations in Crater Morphology," *Icarus*, Vol. 18 (in press).

VIII-25. Kuiper, G. P., "Survey of Asteroids," *Ap. J. Suppl.*, Vol. 3, p. 289, 1958.

VIII-26. Van Houten, C. J., Van Houten-Groeneveld, I., Herget, P., and Gehrels, T., "The Palomar-Leiden Survey of Faint Minor Planets," *Astron. Astrophys. Suppl.*, Vol. 2, p. 339, 1970.

VIII-27. Mutch, T. A., *Geology of the Moon*, Princeton University Press, 1970.

VIII-28. Alexander, W., McCracken, C., and Bohn, J., "Zodiacal Dust: Measurements by Mariner IV," *Science*, Vol. 149, p. 1240, 1965.

VIII-29. Dycus, R. D., "The Meteorite Flux at the Surface of Mars," *Pubs. Astron. Soc. Pac.*, Vol. 81, p. 399, 1969.

VIII-30. Öpik, E. J., "The Stray Bodies in the Solar System. Part I: Survival of Cometary Nuclei and the Asteroids," *Adv. Astron. Astrophys.*, Vol. 2, p. 219, 1963.

VIII-31. Hartmann, W. K., "Paleocrate Ring on the Moon: Review of Post-Apollo Data," *Astrophys. and Space Sci.*, Vol. 17, p. 48, 1972.

VIII-32. Hartmann, W. K., "Terrestrial and Lunar Flux of Large Meteorites in the Last Two Billion Years," *Icarus*, Vol. 4, p. 157, 1965.

VIII-33. Baldwin, R. B., "On the History of Lunar Impact Cratering: The Absolute Time Scale and the Origin of Planetesimals," *Icarus*, Vol. 14, p. 36, 1971.

VIII-34. Shoemaker, E. M., Hackman, R., and Eggleton, R., "Interplanetary Correlation of Geologic Time," *Advances in Astronaut. Sci.*, Vol. 8, p. 70, 1961.

VIII-35. Chapman, C. R., *Topics Concerning the Surfaces of Mercury, Mars and the Moon*, Ph.D. thesis, unpublished, Harvard University, 1967.

VIII-36. Binder, A. B., and Cruikshank, D. P., "Lithological and Mineralogical Investigation of the Surface of Mars," *Icarus*, Vol. 5, p. 521, 1966.

Acknowledgments

Note Added in Proof

Ongoing research and several correspondents have illuminated certain areas of this initial analysis of *Mariner 9* cratering data. The most important area relates to the rate of crater formation on Mars. George Wetherill has pointed out to the author that available Mars-crossing asteroids are poor indicators of the present cratering rate because of the unlikelihood of their actually hitting Mars. Several workers are now assessing new mechanisms for bringing asteroidal fragments into orbits for potential Mars-collision, but no definite estimates of flux rate have yet come from this work. Verne Oberbeck points out that gravitational field differences between Earth, Mars, and the Moon affect crater sizes, introducing an additional small correction to the cratering rate estimated here. The result is that while the relative ages quoted here for Martian provinces and structure are believed to be correct, work now in progress may soon make it possible to improve the estimates of absolute age. There is some suggestion that absolute ages of young features such as the large volcanoes could increase by a factor of 2 or 3. The writer hopes to pursue these problems as new data emerge. He also thanks George McGill for additional comments which have resulted in a number of improvements to the manuscript.